SEMARAK ILMU PUBLISHING

Journal of Advanced Research in Micro and Nano Engineering

Journal homepage:
https://semarakilmu.com.my/journals/index.php/micro_nano_engineering/index
ISSN: 2756-8210

Effect of Nanofillers on the Flexural Performance of 3D Fibre-Reinforced Composites

Mirza Zahid Hussain[1], Syed Zulfiqar Hussain Shah[1,*], Puteri Sri Melor Megat-Yusoff[1], Faiz Ahmad[1], Syed Muhammad Hussnain[1], Rizwan Saeed Choudhry[2], Tahir Sharif[3]

[1] Department of Mechanical Engineering, Universiti Teknologi PETRONAS, 32610 Seri Iskandar, Perak, Malaysia
[2] Department of Mechanical Engineering, University of Doha for Science and Technology, 24449, Doha, Qatar
[3] College of Science and Engineering, University of Derby, Kedleston Rd, Derby, DE22 1GB, United Kingdom

ARTICLE INFO

Article history:
Received 7 July 2024
Received in revised form 13 August 2024
Accepted 28 September 2024
Available online 30 November 2024

Keywords:
3DOWC; nanoparticles; nanostrength M53®; GNP; damage mechanism

ABSTRACT

The aim of this study is to improve the flexural performance and damage mechanism of nano-filled three-dimensional orthogonal woven E-glass/epoxy composites (3DOWC). The inherent brittleness of epoxy-based 3DOWC leads to the early onset of damage mechanisms such as matrix cracking, fibre-matrix debonding, and fibre failure. To overcome these limitations, epoxy resin has been modified with nano-fillers such as graphene nanoplatelets (GNP) and the novel nanostrength® (NS). The epoxy resin was infused in 3DOWC using VARI with different weight percentages of GNP (0.5, 1.0, and 1.5 wt.%) and NS (2.5, 5.0, and 7.5 wt.%). Three samples in each warp and weft direction of 3DOWC were tested in a three-point bend test. The results showed an increase of 48.4%, 56.2%, and 27.4% in flexural strength, final failure, and energy absorption under warp-loading with 0.5 wt.% GNP, respectively, whereas weft-loaded samples with 1.5 wt.% GNP exhibited 12.0% and 10.5% increases in flexural strength and final failure, respectively. However, 7.5 wt.% NS showed an increase in flexural strength in the warp and weft directions by 36.9% and 39.3%, respectively, and an increase in final failure and energy absorption in the warp direction by 39.4% and 12.3%, respectively. For weft-loaded samples, the final failure increased by 39.3% for the same weight percentage, but there was no significant increase in energy absorption in this direction. Scanning electron microscopy (SEM) of damaged samples revealed that crack reconnection by GNP and fibrils formation and plasticization by NS particles improved the overall flexural performance of 3DOWC.

1. Introduction

In recent decades, 3D fibre-reinforced composites (3D-FRCs) standout for their excellent mechanical and physicochemical properties, which offer them a wide range of structural applications across the industries high strength-to-weight ratios with tailored properties are required. The epoxy-reinforced resin systems are widely used to produce 3D-FRCs due to the compatibility with conventional manufacturing processes [1-6]. One of the disadvantages of epoxy-based 3D-FRCs is the

* *Corresponding author.*
E-mail address: syedzulfiqar.shah@utp.edu.my

https://doi.org/10.37934/armne.26.1.1529

fragile appearance of their amorphous matrix under mechanical stress, which is mainly due to its inherent brittleness. This brittleness would lead to the initiation of damage mechanisms such as matrix cracking, fibre-matrix debonding, delamination, and fibre breakage [7,8]. To overcome these early damage mechanisms, matrix modification by adding inorganic modifiers (Al_2O_3, SiO_2, BN, kaolinite, smectite), organic modifiers (GNPs, carbon nanotubes (CNTs)), elastomeric modifiers (core-shell rubber (CSR)), and phase separating modifiers (block copolymers (BCP)), with the aim of improving their toughness had been identified as a cost-effective technique [9-13].

Vaganov *et al.,* [14] found that by incorporating 1.0 wt.% CNTs into carbon fibre (CF) -reinforced epoxy resin composites, their flexural strength increased by 13.3%, with improved fibre bridging and fibre pull-out mechanisms, providing additional energy for crack initiation and propagation compared to neat epoxy matrix composite. Yildirim *et al.,* [15] found that the addition of CNTs to 3D glass fibre (GF)-reinforced epoxy composites increased their flexural strength in the warp and wept directions by 25% and 44%, respectively. The authors also showed that the uniform distribution of CNTs provided good interfacial bonding between fibre and matrix, leading to an improvement in damage mechanisms. Panchagnula and Kuppan [9] studied that the flexural strength of GF/epoxy resin composites with 0.3 wt.% addition of multiwall carbon nanotubes (MWCNT) increased by 39.41% compared to the pristine samples with improved damage mechanisms. Xu and Hoa [16] found a 38% improvement in flexural strength by incorporating only 2 wt.% of nanoclay into CF-reinforced epoxy resin composites.

Kumar *et al.,* [11] summarized that GF-reinforced epoxy composites with 2 wt.% nanoclay exhibited a significant increase in flexural strength and modulus by 38% and 110.4%, respectively, and showed improved surface morphologies. The damage mechanisms such as agglomeration, shear failure and crack propagation within the GNP layers [17,18], prompt the researcher to modify epoxy resin with phase-separating modifiers such as BCP [19]. The Nanostrength® M53, a tri-block copolymer (M-A-M) developed by Arkema company, which consists of a centered polybutylacrylate (PBuA) block surrounded by two blocks of polymethylmethacrylate (PMMA), can be miscible with polymer resins and offers good improvement to crack initiation and propagation under flexural load. Kouassi *et al.,* [20] showed that 10 wt.% NS (M53)-modified bi-directional glass fibre with thermoplastic resin (Elium) exhibited improved damage mechanisms such as fibre-matrix debonding, fibre pull-out and fibre failure. Wang *et al.,* [21] added 3.5 to 6.7 wt.% of Di-BCP to the epoxy resin to increase the flexural strength and found a significant improvement in fracture toughness. Bashar *et al.,* [22] revealed that epoxy resin modified with 5 wt.% Nanostrength (NS) acrylic tri-BCP (M52, M52N) had improved damage mechanisms.

Several studies have highlighted that uniform dispersion, agglomeration, surface treatments, incompatibility between blocks due to the random sequence of monomers and plasticity of nano-fillers can influence the final mechanical properties of 3D-FRC [23-25]. Following these directions, this study focused on improving the flexural performance and damage mechanisms of epoxy-based 3DOWC using nanofillers i.e., GNP and NS. Modified epoxy resins with different concentrations of nano-fillers were prepared and used as a matrix to fabricate 3D-FRCs using vacuum-assisted resin infusion (VARI) method. First, 3DOWC was fabricated with pristine epoxy matrix and toughened epoxy matrix reinforced with different concentrations of GNP (0.5, 1.0, and 1.5 wt.%) and NS (2.5, 5.0, and 7.5 wt.%). Second, flexural tests were carried out along the warp and weft directions to evaluate the effect of nanoparticles on the flexural performance of 3D-FRCs. Finally, scanning electron microscopy (SEM) was performed on pristine, single nano-filled 3DOWC damaged samples to investigate the improvement in damage mechanisms by the addition of nanoparticles. This work aims to make an important contribution to understanding the flexural performance and failure

mechanisms of nano-filled 3D-FRCs. This information can be helpful for the engineering and structural applications of these composites.

2. Methodology

2.1 Material Used

A 3D orthogonal E-glass woven fabric (3D-9871) purchased from Textech® Industries, USA was used in this study, as shown in Figure 1(a). This fabric consists of three warp layers and four weft layers held together by a through-thickness reinforcement, that moves along the warp direction, as shown in the schematic diagram in Figure 1(b). The overall thickness of a single-layer dry fabric is approximately 4.3 mm with an aerial density of 5200 GSM. Thermoset epoxy resin system Epolam® 2040 and the hardener Epolam® 2042 supplied by from Axson, China was used in ratio 100:30 by weight to fabricate 3DOWC panels. To improve the toughness of the epoxy resin, commercial grade ABA type acrylic Tri-BCP (Nanostrength®) M53 with a size of approximately 10-100 nm (nano-filler) from Arkema, France, and GNP with a size of approximately 2-8µm (micro-filler) provided by Sigma-Aldrich (M) Sdn. Bhd., Malaysia, added.

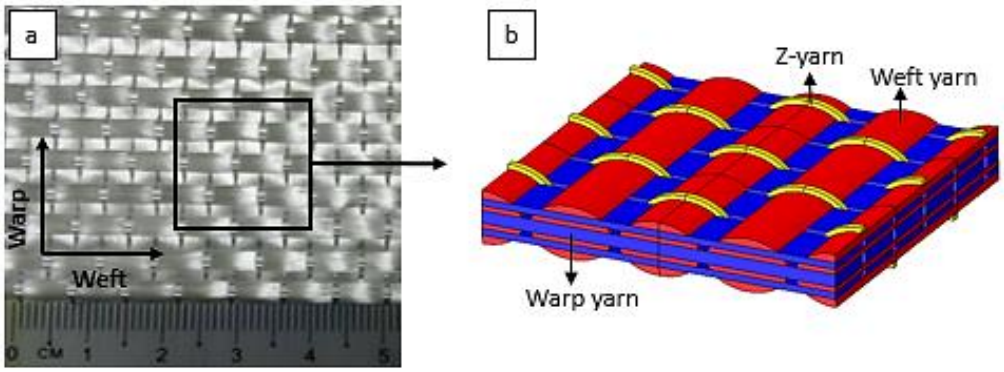

Fig. 1. 3D fibre-reinforced composite (a) 3D E-glass orthogonal woven fabric (3D-9871) used for the fabrication of composites samples (b) Schematic diagram of 3D orthogonal fabric (blue, red, and yellow colors represent warp, weft, and z-yarn, respectively)

In this study, the weight percentages of GNP (0.5, 1.0, and 1.5 wt.%) and NS (2.5, 5.0 and 7.5 wt.%) were used as nano-fillers to improve the flexural performance and damage mechanisms of 3DOWC. The mechanical and physical properties of Epolam® resin 2040, Epolam® hardener 2042, and GNP, NS (M53) are summarized in Table 1.

Table 1
Summary of mechanical and physical properties of the material

Material	Properties	Values
Fabric [26-30]	Fabric	3D orthogonal E-glass woven fabric
	Orientation	$[0^0/90^0]$
	Thickness	~ 4.3 mm
	Weight	5200 GSM
Epolam® resin 2040 [31]	Aspect	Liquid
	Colour	Light amber
	Density at 25 ℃ (g/cc)	1.16
	Viscosity at 25 ℃ (mPa.s)	1300
	Elongation at failure (%)	8.7
	Flexural modulus (MPa)	2900

	Flexural strength (MPa)	125
	Tensile strength (MPa)	75
	Tensile modulus (GPa)	3.1
Epolam® hardener 2042 [31]	Aspect	Liquid
	Colour	Light amber
	Density at 25 ℃ (g/cc)	0.95
	Elongation at break (%)	8.7
	Viscosity at 25 ℃ (mPa.s)	15
Graphene nanoplatelets (GNP) [32]	Aspect	Powder
	Colour	Dark grey to black
	Bulk density	0.03-0.1 g/cm^3
	Particle size	2-8 μm
	Surface area	50-80 m^2/g
	Acid content	$\leq 0.5\%$
Nanostrength® M53 [33]	Aspect	Solid
	Colour	Light yellow
	Particle size	10-100 nm

2.2 Fabrication Process

The VARI method was used to fabricate the pristine, NS-based, and GNP-based 3DOWC, as shown in Figure 1(c). Six types of single nano-filled 3DOWC panels were prepared with a size of 280 mm×250 mm with three different concentration levels of each NS (2.5 wt.%, 5.0 wt.% and 7.5 wt.%) and GNP (0.5 wt.%, 1.0 wt.% and 1.5 wt.%). Before infusion, the 3D fabric was dried in an oven at 125 °C for two hours and the resin was prepared for NS-based and GNP-based epoxy system, respectively, as per the procedure explained in Figures 2(a) and 2(b). In the case of pristine epoxy based 3DOWC; epoxy resin and hardener in weight ratio (100:30) were carefully mixed for ten minutes to obtain a homogeneous mixture. The mixture was degassed for ten minutes to avoid deterioration of the final mechanical properties due to an increase in void content. Then the resin was infused, which takes almost 6-7 minutes to complete the infusion process.

In the case of NS-based 3DOWC, Figure 2(a) provides an overview of the resin preparation procedure for infusion. Firstly, resin (70%) and wt.% NS (2.5, 5.0, and 7.5 wt.%) were mechanically stirred at 100-120 rpm and 300 °C for 1 hour to achieve complete dissolution of the NS particles. The hardener (30%) was then mixed and mechanically stirred for 20 minutes to obtain a uniform and homogeneous mixture. Lastly, the mixture was degassed for ten minutes to remove the air bubbles and infused to prepare NS/epoxy-based 3DOWC.

Furthermore, Figure 2(b) explains the resin preparation process for the fabrication of GNP-based 3DOWC panels. First, GNP was mechanically mixed with solvent (absolute ethanol 99.9%; BDH 20821-321) followed by exfoliation in a closed glass beaker using an ultrasonic bath (model: 040S, 240 W power and 40 kHz frequency) at 30-80 ℃ for 1 hour to achieve an even distribution of the GNP. After sonication, the GNP/ethanol solution was heated to 100-120 ℃ on the hot plate in an open beaker to completely evaporate the ethanol and leave the dried GNP powder. *Next*; the hardener (30%) and GNP (0.5, 1.0, and 1.5 wt.%) were manually mixed for 20 minutes to obtain a homogeneous solution. Finally, the obtained mixture was mixed with resin (70%) for 20 minutes followed by the degassing of resin before infusion.

During the infusion process, mesh and peel ply were used on both sides of the 3D fabric to achieve uniform distribution of the nano-fillers. The VARI process was performed at 600 mbar to avoid boiling of the resin, and the infusion process was completed in 7 and 15 minutes for GNP-based and NS-based epoxy system, respectively, as shown in Figure 2(c). More details on the fabrication process can be found in previous work [34-37]. After completing the polymerization process at room

temperature, the panels were post-cured in an oven at 80 ℃ for eight hours to achieve their maximum mechanical properties.

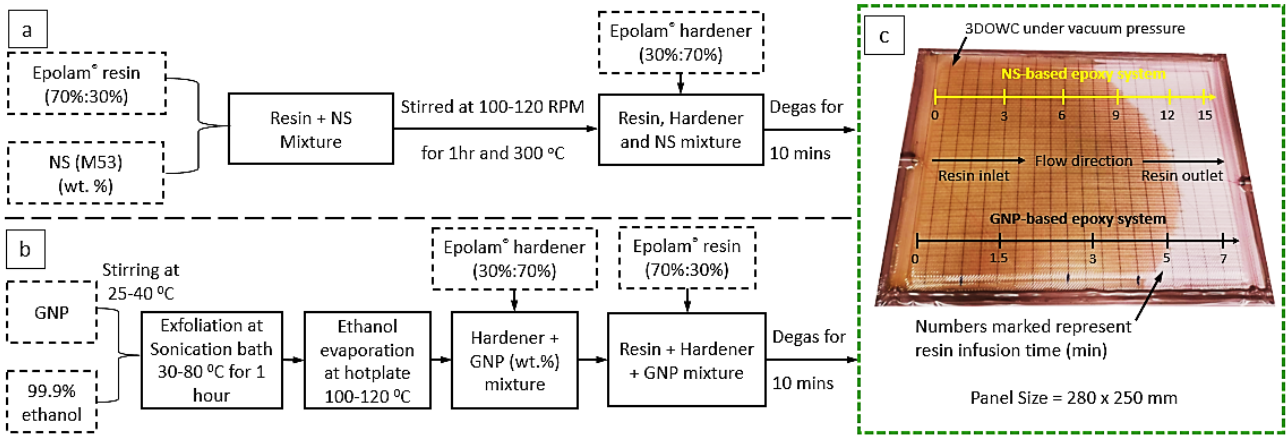

Fig. 2. Flowchart for resin preparation and fabrication process of composite panels (a) NS-based epoxy system (b) GNP-based epoxy system (c) Vacuum infusion process along with vacuum infusion time for NS- and GNP-based epoxy system (numbers marked represent resin infusion time in minutes)

2.3 Physical Parameters of the Cured Panels and Samples

After the panels were fully cured, the samples were cut from each panel using a water-based diamond cutter, which gives an excellent surface finish. The physical parameters such as density, fibre volume fraction (FVF), void content (VC) and thickness (t) of the average of five samples for each configuration were measured [38,39]. The density of the samples was measured according to ASTM D792-08 [40], and FVF and VC were measured using ASTM D3171-15 [41]. The average values of density, FVF, VC and thickness with their standard deviations are summarized in Table 2. For all samples, the FVF was found to be less than 55% and the VC less than 5%, as shown in Figures 3(a) and 3(b), respectively.

Table 2
Physical parameters for 3DOWC with pure epoxy and single filler (average of five samples). ρ: density, V_f: fibre volume fraction, V_m: matrix volume fraction, VC: void content, t: thickness

Nomenclature	Material	ρ (g/cc)	V_f (%)	VC (%)	t (mm)
Pristine 3DOWC	Pure epoxy	1.88 ± 0.02	54.0 ± 1.1	1.8 ± 1.0	3.89 ± 0.07
S1	0.5 wt. % GNP	1.86 ± 0.01	53.1 ± 0.89	2.3 ± 0.4	3.87 ± 0.06
S2	1.0 wt. % GNP	1.87 ± 0.01	54.9 ± 0.5	3.9 ± 0.2	3.88 ± 0.08
S3	1.5 wt. % GNP	1.88 ± 0.02	54.9 ± 1.14	2.4 ± 0.6	3.89 ± 0.09
S4	2.5 wt. % NS	1.89 ± 0.01	54.7 ± 1.17	1.4 ± 0.4	3.95 ± 0.08
S5	5.0 wt. % NS	1.85 ± 0.02	51.9 ± 1.06	2.2 ± 0.8	3.93 ± 0.05
S6	7.5 wt. % NS	1.86 ± 0.03	52.6 ± 1.46	1.9 ± 0.6	4.08 ± 0.08

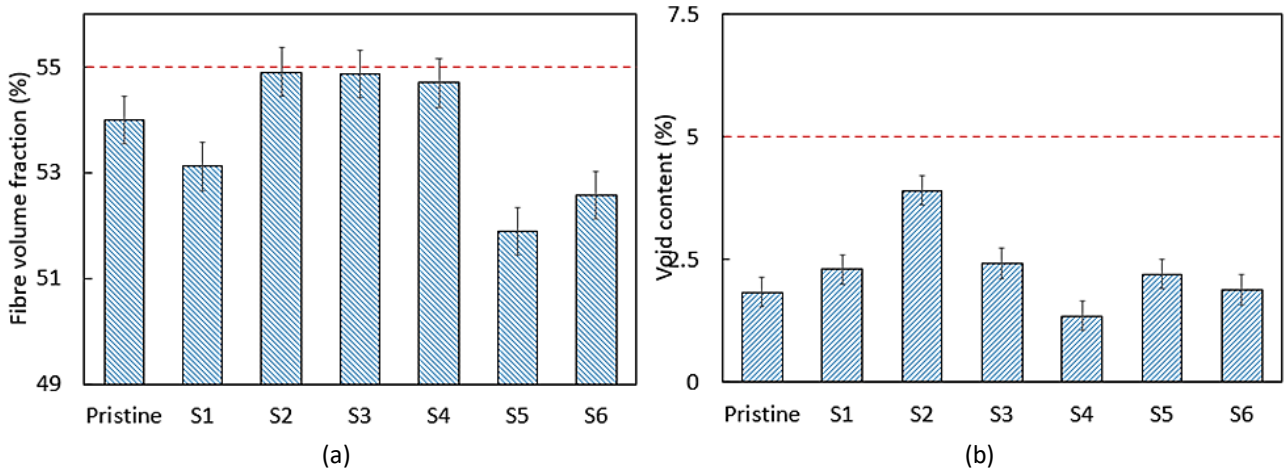

Fig. 3. Comparison of physical parameters for 3DOWC (a) Fibre volume fraction (FVF) (b) Void content (VC)

2.4 Flexural Testing

The flexural test was conducted according to ASTM D7264 (procedure A, three-point bending) [42], using a GoTech Universal Testing Machine (UTM) equipped with a 5 kN load cell [43]. The flexural tests were carried out in each warp and weft direction on a three-point bending fixture with a fixed span of 64 mm. A total of 42 rectangular samples were prepared (each sample has a dimension 80 mm × 25 mm × 4 mm), i.e., 6 samples for pristine 3DOWC, 18 for GNP-based 3DOWC, and 18 for NS-based 3DOWC. Three samples were tested in each warp and weft direction at a constant loading rate of 1 mm/min. If the standard deviation between three samples tested was greater than 10%, additional samples were tested for that configuration to reduce the standard deviation to 10% or less. The flexural strength, modulus, and deflection properties were measured during the flexural test. The flexural strength (σ_f), flexural modulus (E_f) and flexural strain (ε_f) can be calculated by using the Eqs. (1), (2) and (3) respectively.

$$\sigma_f = \frac{3FL}{2bd^2} \tag{1}$$

$$E_f = \frac{L^3}{4bd^3}\frac{\Delta P}{\Delta \delta} \tag{2}$$

$$\varepsilon_f = \frac{6\sigma d}{L^2} \tag{3}$$

where "L" , "b" , "d" , "ε" and "F" represent the span, width, thickness, and applied load, respectively, while “ΔP” and “Δδ” represent load increments and deflection increments.

2.5 Failure Mechanisms

To better understand the damage mechanisms in 3DOWC, scanning electron microscopy (SEM) was performed on cross-sections obtained from damaged samples for each pristine, GNP-based, and NS-based 3DOWC. The SEM machine ZEISS-SUPRA 40 VP was used for the analysis. A water-based diamond disc precision cutter was used to cut the damaged samples from the mid plane. To obtain high-resolution images, the samples were first polished using a Phoenix 4000 polisher/grinder and then coated with 40 nm gold to improve conductivity. The voltage and maximum magnification used during SEM analysis are 10 keV and 5000×, respectively. A total of six cross sections were examined

using SEM, i.e., two cross sections for each warp and weft direction of pristine 3DOWC, two for GNP-based and two for NS-based 3DOWC.

3. Results

In this section, the flexural performance of GNP-based (0.5 to 1.5 wt.%) and NS-based (2.5 to 7.5 wt.%) 3DOWC is discussed in terms of flexural strength, flexural modulus, final failure (at 50% load drop) and energy absorption in the warp and weft directions.

3.1 Comparison of Stress-Strain Curves for Nano-Filled 3DOWC

The flexural stress-strain curves of GNP-based 3DOWC and NS-based 3DOWC are shown in Figures 4(a) to 4(c) and Figures 4(d) to 4(f), respectively. The stress-strain curves provide comprehensive information about the damage process of 3DOWC under flexural load. Each stress-strain curve in Figure 3 represents the warp (0^0) and the weft (90^0) directions, demonstrating that the flexural properties were sensitive in both directions. All stress-strain curves initially show a linear response, followed by a non-linear behaviour after 1% to 1.5% of the flexural strain. The samples in warp direction have a higher flexural stiffness and load bearing capacity than the samples in the weft direction. Each stress-strain curve exhibits linear behaviour up to a maximum value (ultimate strength), followed by a sudden drop in load caused by the failure of the tensile fibre at the bottom surface of the sample. This brittle behaviour of the samples is due to fibre dominant properties, and a similar observation was made by Shah *et al.,* [2].

The stress-strain curves for 0.5 wt.% GNP are shown in Figure 4(a). In the warp direction, the flexural strength showed a significant increase in stiffness and strength compared to the pristine epoxy-based 3DOWC (194 MPa). The interaction between GNP and epoxy resin helps to improve the load transfer, stiffness, and strength. However, when the GNP content increases to 1.0 wt.% and 1.5 wt.% (Figures 4(b) and 4(c)), the flexural strength decreases, maybe due to the agglomeration and uneven stress distribution. The flexural strength was also slightly increased in the weft direction compared to the pristine 3DOWC (328 MPa). However, the increase in stiffness and strength may be less pronounced than in the warp direction due to differences in fibre orientation, consistent improvement, and better stress distribution.

The comparison of flexural stress-strain curves for NS (2.5 to 7.5 wt.%) in warp and weft directions is shown in Figures 4(d) to 4(f). All stress-strain curves showed a linear response until they approach the elastic limit before plastic deformation and fibre failure. In the warp direction, the flexural strength showed an inconsistent trend across different weight percentages, with the highest flexural strength observed at 7.5 wt.%, followed by 2.5 wt.% and 5.0 wt.%. The higher flexural strength of 7.5 wt.% may indicate an effective interfacial interaction or a well-defined phase morphology of NS. However, a very consistent trend was evident in weft loaded specimens; with increase in NS content, the flexural strength also increases, highest at 7.5 wt.%, followed by 5.0 wt.% and 2.5 wt.%. The weft-loaded samples have higher bending stiffness and peak flexural strength compared to the warp-loaded samples due to the presence of warp yarns on the top and bottom surfaces of the specimens, which resist flexural loads.

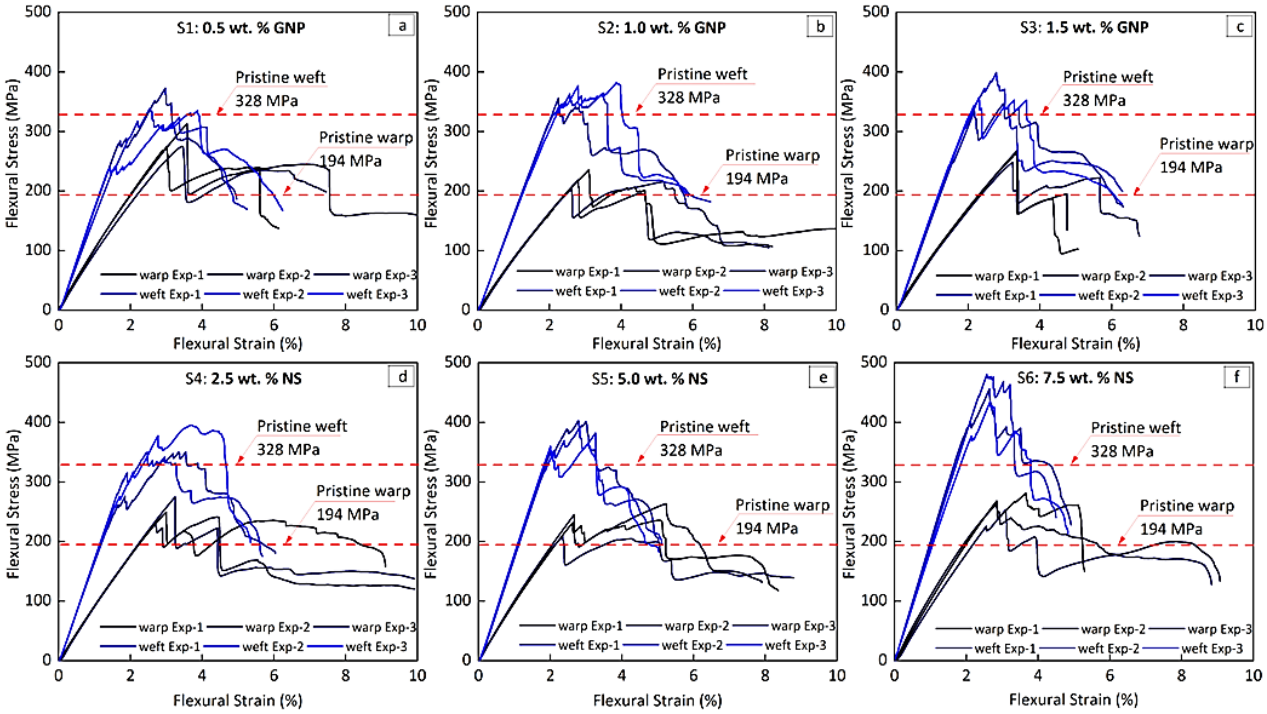

Fig. 4. Stress vs strain curves for nano-filled 3DOWC (a) 0.5 wt.% GNP (b) 1.0 wt.% GNP (c) 1.5 wt.% GNP (d) 2.5 wt.% NS (e) 5.0 wt.% NS (f) 7.5 wt.% NS. Warp: 00 direction, weft: 900 directions

3.2 Comparison of Normalized Flexural Response for Single Nano-Filler

The results obtained from flexural tests in terms of flexural strength, flexural modulus, final failure (50% load drop), and energy absorption are summarized in Table 3. The flexural strength of pristine epoxy-based 3DOWC in the warp and weft directions was 194 MPa and 328 MPa, respectively. For GNP/epoxy resin 3DOWC, the warp-loaded samples showed higher flexural strength at low concentration, while the weft-loaded samples appeared at higher GNP concentration, as shown in Figures 5(a) and 5(b). The flexural strength in the warp and weft directions was increased by 48.4% and 12.0% at 0.5 wt.% and 1.5 wt.% GNP compared to pristine epoxy-based 3DOWC, respectively, while the flexural modulus remains constant, as illustrated in Figures 5(c) and 5(d).

Table 3
Summary of test results for single filler (average of 3 tested specimen of each case)

Configuration		Flexural strength (MPa)	Flexural modulus (GPa)	Final failure (50% load drop) (N)	Energy absorption (J)
Pristine	warp	194±8.6	9±0.4	8±0.8	388±9.3
	weft	328±9.1	16±1.5	11±1.4	677±8.3
S1	warp	288±9.0	10±0.4	11±3.1	606±8.7
	weft	349±8.7	17±0.9	9±1.0	727±2.9
S2	warp	223±10.2	9±0.2	9±2.0	457±4.2
	weft	368±3.1	16±0.6	10±0.5	741±9.8
S3	warp	260±9.8	9±0.1	6±1.5	538±6.2
	weft	368±7.9	16±0.3	10±0.2	748±1.7
S4	warp	255±6.8	9±0.1	11±0.9	514±4.4
	weft	365±6.0	17±0.4	10±0.3	732±7.5
S5	warp	236±7.4	10±0.3	11±1.4	493±0.2
	weft	387±9.2	18±0.3	9±0.3	768±6.2
S6	warp	265±3.7	10±0.5	9± 2.0	541±4.4
	weft	457±2.7	19±1.0	10±0.4	943±5.2

Subsequently, the high GNP concentration could lead to the agglomeration of nanoparticles, which could reduce the flexural strength due to the generation of localized stress concentration that serves as initiation point for crack formation and propagation. Conversely, lower GNP concentrations can result in higher flexural strength due to the uniform dispersion of GNP throughout the matrix, thereby providing the nucleation sites for crack deflection and retention. In terms of final failure (50% load drop) and energy absorption, the warp-loaded samples show an increase in final failure and energy absorption of 56.2% and 27.4%, respectively at 0.5 wt.% GNP; however, the weft-loaded samples show a 10.5% increase in final failure at 1.5 wt.% GNP and no significant increase in energy absorption in this direction.

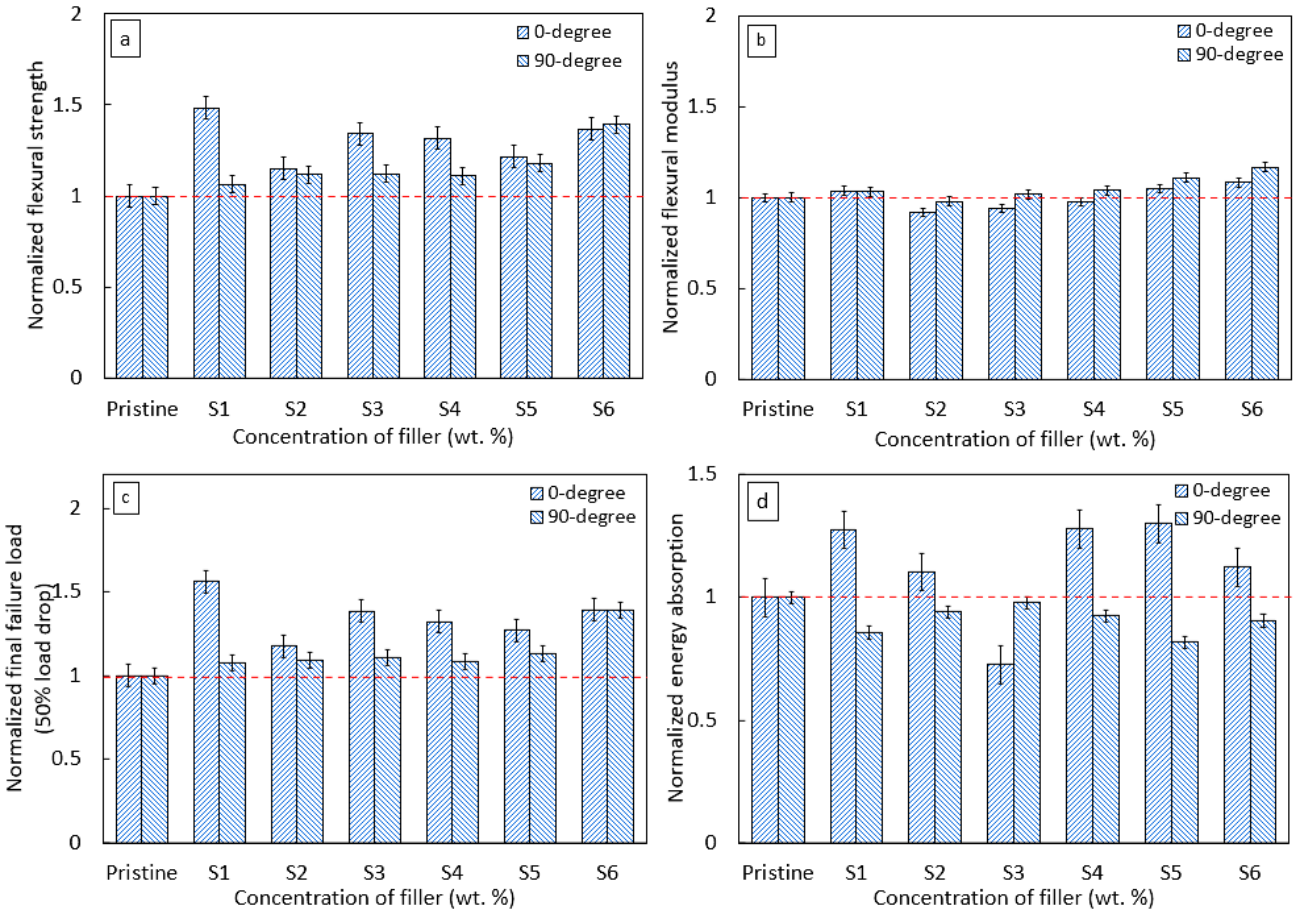

Fig. 5. Comparison of normalized response for nano-filled 3DOWC (a) Flexural strength (b) Flexural modulus (c) Final failure load (50% load drop) (d) Energy absorption, in warp (0°) and weft (90°) direction

In contrast, the NS/epoxy system showed an increase in flexural strength with an increase in NS concentration. The flexural strength increased by 36.9% and 39.3% at 7.5 wt.% NS in the warp and weft directions, respectively, with a slight increase in the flexural modulus by 8.3% and 16.6%, respectively, compared to the pristine 3DOWC samples, as shown in Figures 5(a) and 5(b). In terms of final failure (50% load drop) and energy absorption; at 7.5 wt.% NS, the warp-loaded samples showed a 39.4% and 12.3% increase in final failure and energy absorption, respectively, whereas the weft-loaded samples exhibited a 39.3% increase in final failure and no significant increase in energy absorption in this direction, as depicted in Figures 5(c) and 5(d). The increase in flexural strength by modifying epoxy resin with NS could be due to the better adhesion between fibre and matrix interface, self-assemble linkage into nanostructures and unique morphology of Nanostrength®. The M53 (NS) block copolymer consists of two PMMA blocks and a PBuA core. The PMMA block forms an

effective shell around the epoxy resin and the PBuA core provides an immiscible rubber phase that stretches under the flexural load. Therefore, an increase in the NS concentration results to an increase in the flexural strength, final failure, and energy absorption in the 3DOWC.

3.3 Damage Mechanism

In the following section, detailed failure mechanisms in 3D-FRCs under flexural loading and the corresponding improvements through matrix modification are presented using SEM images.

3.3.1 Damage morphologies in pristine 3D-FRCs

Figure 6 shows the SEM images of microscopic damage mechanisms in the epoxy-based 3D-FRCs under flexural loading. The main damage mechanisms in the epoxy-based 3D-FRCs were matrix cracking, debonding/ delamination of the fibre-matrix interface, yarn tensile failure, yarn kinking, and re-orientation of yarns. The increase in micro-crack size and density leads to the formation of stress concentration regions, contributes to the development of macro-cracks within the matrix. Figures 6(a) and 6(b) shows debonding and failure of the fibre-matrix interface due to the weak interfacial bonding, localized deformation of the epoxy matrix, and inadequate impregnation or resin-rich areas. Fibre tensile failure occurs near the bottom surfaces of the samples which are induced by the stress concentrations and flexural loads, wherein high stresses along the outer fibers exceed their tensile strength, as highlighted in Figure 6(c). Furthermore, matrix micro-cracking and re-orientation of yarn leads to the formation of kinking band and extensive interface failure. These kinking bands serve as sites for crack initiation, as shown in Figure 6(d).

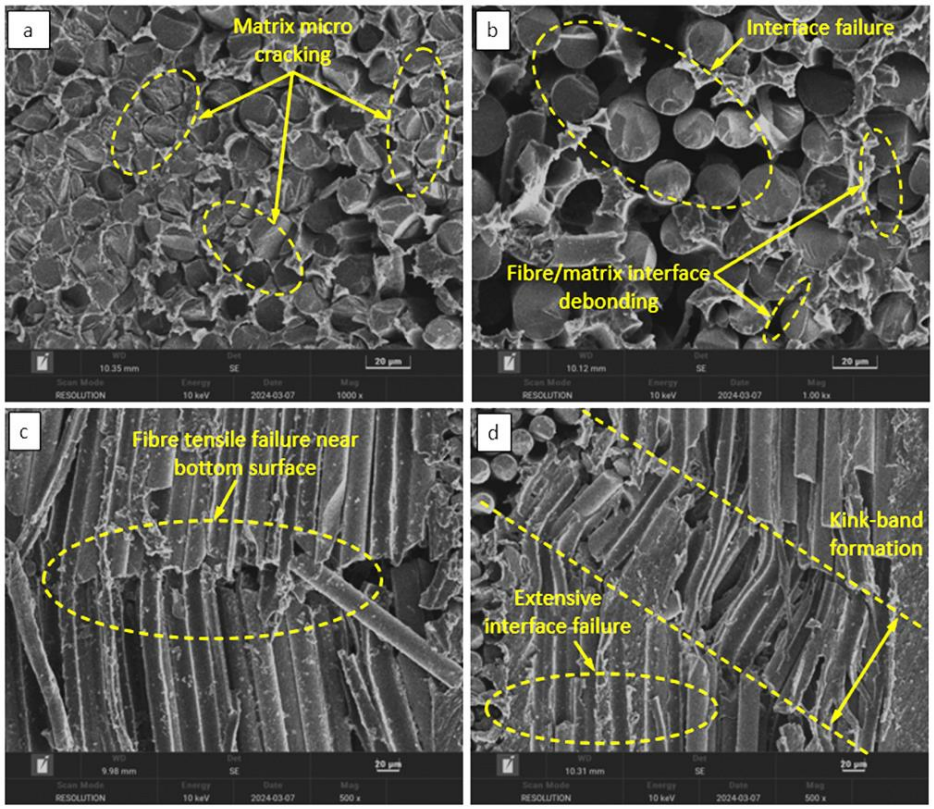

Fig. 6. The failure process morphology (SEM images) for pristine 3DOWC (a) Micro matrix cracking (b) Fibre-matrix interface debonding (c) Fibre tensile failure near the bottom surface (d) Fibre kinking and failure

3.3.2 Damage morphologies in nano-filled 3D-FRCs

The flexural loaded cross-section of GNP/epoxy and Nanostrength® (M53)/epoxy-based 3D-FRCs were examined for micro-structural analysis using SEM, as shown in Figure 7 and Figure 8, respectively. In GNP-based 3DOWC, crack pinning or bifurcation, crack deflection and separation between GNP layers are the main damage mechanisms. First, microcrack pins near the GNP particle, then they face the GNP agglomerates, which form branches of the main microcrack. This crack redirection prolongs matrix cracking and delays delamination of the fibre-matrix interface resulting in a tougher fibre-matrix interface compared to pristine epoxy-based 3DOWC. On the other hand, these branched microcracks re-connect with some variation of their height, resulting in shear failure of the GNP particles in the matrix, as shown in Figures 7(a) and 7(b). Evidence for such a crack pinning mechanism was also reported by Bortz *et al.,* [17]. The second major damage mechanism results from the separation of the GNP layers. The cracks captured by the GNP particle create a separation between their layers, which eventually connects the main branching cracks. This layer separation influences the microstructure of the GNP-based matrix resin. A similar phenomenon was also reported by Parashar and Mertiny [18]. Therefore, low GNP loading can lead to a harder fiber-matrix interface by bridging cracks and avoiding agglomerates, whereas a higher loading leads to stronger layer separation, as shown in Figures 7(c) and7(d).

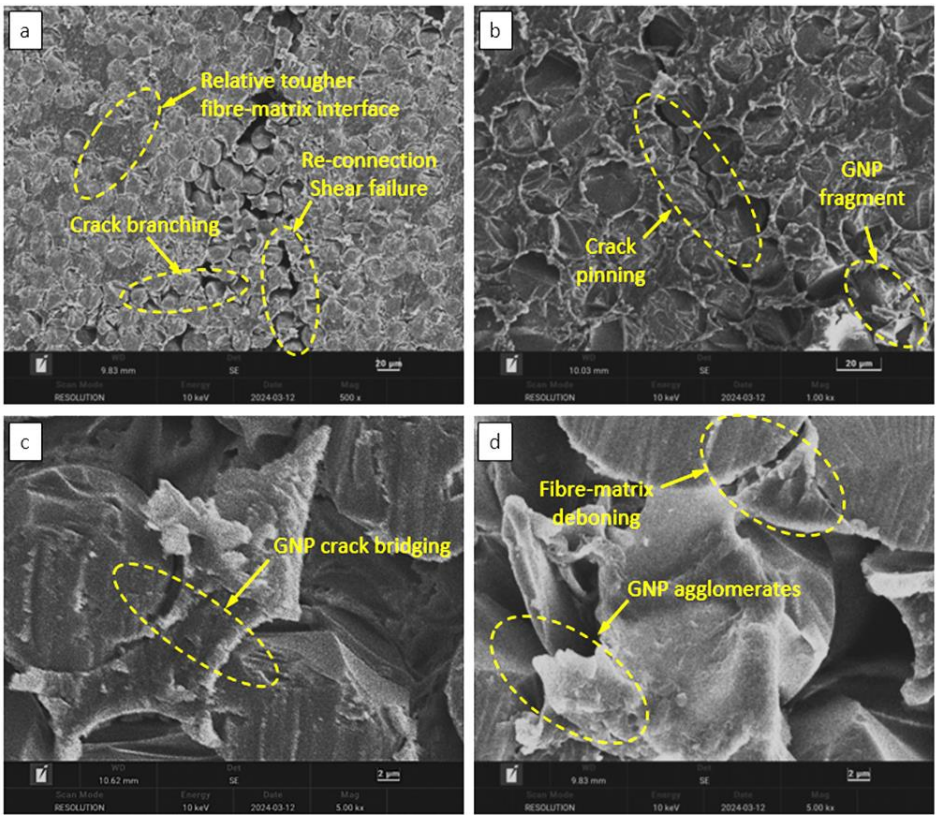

Fig. 7. Damage morphology for GNP modified 3DOWC (a) Crack branching and reconnection (b) GNP fragment and crack pinning (c) Crack bridging (d) GNP agglomerates

While in NS-based 3DOWC, damages mechanisms occur in BCP-rich regions due to crack pinning, particle stretching, partial debonding and formation of fibrils or strands, as explained using SEM images in Figure 8. The tougher fibre-matrix interface was revealed due to the strong interfacial bonding and microphase separation, as shown in Figure 8(a). The NS particles act as barriers to crack

propagation, deflecting the crack path and increasing the plasticity of the matrix, as shown in Figure 8(b). Therefore, the interface between NS and matrix requires more energy for the further propagation of microcracks. The crack bridging by the NS particle includes their stretching, partial debonding and the creation of a cup and cone shape. Thus, the dispersed spherical tri-block copolymer nanoparticles in interconnected domains induce robust toughening mechanisms such as plastic deformation and bridging, as shown in Figures 8(c) and 8(d), a similar phenomenon was also reported by Klingler and Wetzel [44].

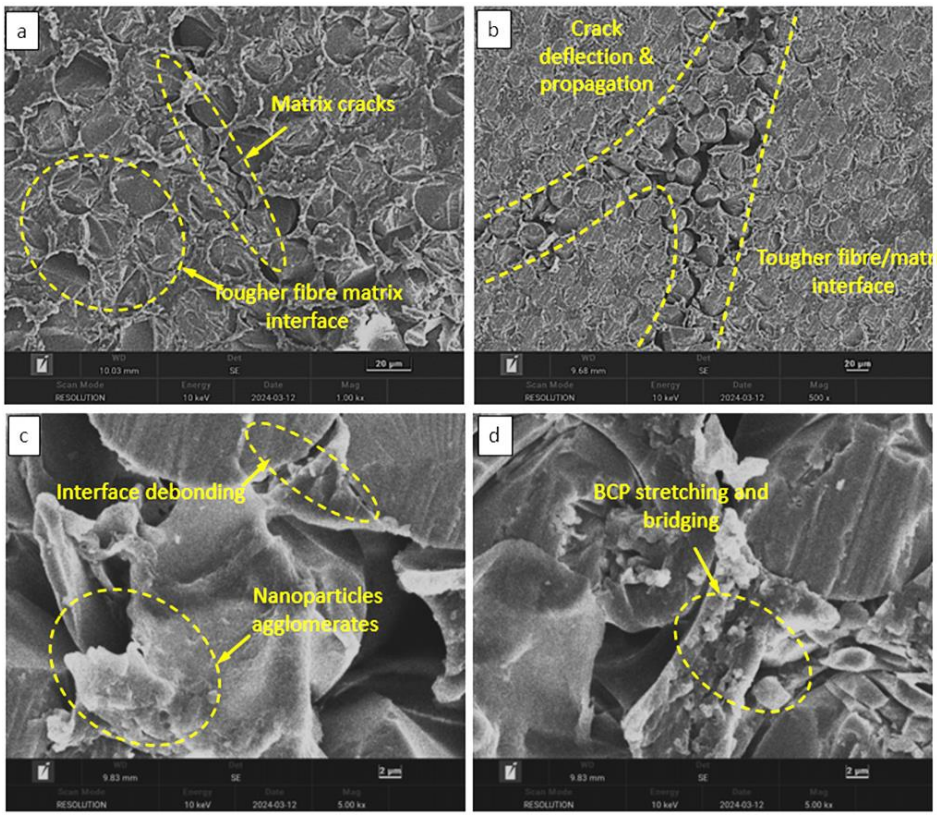

Fig. 8. Damage morphology for NS modified 3DOWC (a) Micro matrix cracking (b) Crack deflection and propagation (c) Fibre-matrix interface debonding (d) BCP stretching and bridging

4. Conclusions

Modification with nanoparticles influences the flexural performance, damage mechanism, and final failure mode of 3DOWC. This presented tailored matrix modification approach investigated a detailed analysis of the nanofillers (NS and GNP) for the flexural properties and damage mechanisms of 3DOWC. The panels were fabricated by using the VARI method to achieve uniform distribution of nano-fillers and uniform thickness of the samples. For each configuration, three samples were subjected to the three-point bend test in each warp and weft direction. The samples loaded with 0.5 wt.% GNP showed higher flexure strength and final failure in the warp direction due to the uniform dispersion and effective reinforcement of the matrix between the warp fibre, while 1.5 wt.% GNP showed higher flexure strength in weft the direction due to the increased interaction between GNP and the weft fibre. The 0.5 wt.% GNP showed a 48.4% and 56.2% increase in flexural strength and final failure (at 50% load drop) in warp direction as compared to pristine epoxy-based system, whereas in the weft direction, 1.5 wt.% of GNP acquired to increase flexural strength and final failure by 12.0% and 10.5%, respectively. On the other hand, it was found that the energy absorption was

increased by 27.4% at 0.5 wt.% GNP, and there was no significant increase in weft direction. While the NS/epoxy system showed a 36.9% increase in flexural strength at 7.5 wt.% NS in the warp direction and a 39.3% increase in the weft direction. For the warp-loaded samples of the same concentration, final failure and energy absorption increased by 39.4% and 12.3%, respectively. For the weft-loaded samples, final failure increased by 39.3%, but there was no significant increase in energy absorption in this direction.

The enhancement of flexural strength and final failure in both directions due to their ability of cross-linkage, self-assemble into nanostructures, uniform dispersion, and plasticization. The damage mechanism attributed by the modification of GNP evidence of crack deflection and crack pinning. In addition, important damage mechanisms are separation between the GNP layers that occurs at multiple places and shear within the GNP layer due to weak force between GNP layers. It is also evident that these separations which occur at multiple places can also combine to the main crack. However, the mechanism of separation within the sheets can either be shear or rapture of GNP particle depending on the orientation of the sheet to the load and crack propagation direction. On the other hand, the modification with NS attributes the particle stretching, crack bridging and debonding, formation of fibrils or strands, matrix plasticization, and strong adhesion between fibre and matrix. The NS particles were homogenously dispersed throughout the matrix.

Acknowledgement

The authors would like to acknowledge the financial support provided by Universiti Teknologi PETRONAS (015LC0-351). The author would also like to acknowledge the support of Sharp Keith from Textech Industries for providing the 3D fabric for this research work. The authors are grateful to Pierre Gerard from Arkema for providing Nanostrength® for this research work.

References

[1] Liu, Gang, Kai Huang, Yucheng Zhong, Zhixing Li, Hongjun Yu, Licheng Guo, and Shuxin Li. "Investigation on the off-axis tensile failure behaviors of 3D woven composites through a coupled numerical-experimental approach." *Thin-Walled Structures* 192 (2023): 111176. https://doi.org/10.1016/j.tws.2023.111176

[2] Shah, Syed Zulfiqar Hussain, Puteri SM Megat-Yusoff, Saravanan Karuppanan, Rizwan Saeed Choudhry, and Zubair Sajid. "Off-Axis and on-axis performance of novel acrylic thermoplastic (Elium®) 3D fibre-reinforced composites under flexure load." *Polymers* 14, no. 11 (2022): 2225. https://doi.org/10.3390/polym14112225

[3] Shah, S. Z. H., and Juhyeong Lee. "Stochastic lightning damage prediction of carbon/epoxy composites with material uncertainties." *Composite Structures* 282 (2022): 115014. https://doi.org/10.1016/j.compstruct.2021.115014

[4] Guo, Qiwei, Yifan Zhang, Ruiqing Guo, Ming Ma, and Li Chen. "Influences of weave parameters on the mechanical behavior and fracture mechanisms of multidirectional angle-interlock 3D woven composites." *Materials Today Communications* 23 (2020): 100886. https://doi.org/10.1016/j.mtcomm.2019.100886

[5] Shah, S. Z. H., S. Karuppanan, P. S. M. Megat-Yusoff, and Z. Sajid. "Impact resistance and damage tolerance of fiber reinforced composites: A review." *Composite Structures* 217 (2019): 100-121. https://doi.org/10.1016/j.compstruct.2019.03.021

[6] Hussnain, S. M., S. Z. H. Shah, P. S. M. Megat-Yusoff, and M. Z. Hussain. "Degradation and mechanical performance of fibre-reinforced polymer composites under marine environments:–A review of recent advancements." *Polymer Degradation and Stability* (2023): 110452. https://doi.org/10.1016/j.polymdegradstab.2023.110452

[7] Shah, S. Z. H., P. S. M. Megat-Yusoff, Tahir Sharif, Syed Zahid Hussain, and R. S. Choudhry. "Off-axis tensile performance of notched resin-infused thermoplastic 3D fibre-reinforced composites." *Mechanics of Materials* 175 (2022): 104478. https://doi.org/10.1016/j.mechmat.2022.104478

[8] Han, Wenqin, Jinyu Zhou, and Qinghe Shi. "Research progress on enhancement mechanism and mechanical properties of FRP composites reinforced with graphene and carbon nanotubes." *Alexandria Engineering Journal* 64 (2023): 541-579. https://doi.org/10.1016/j.aej.2022.09.019

[9] Panchagnula, Kishore Kumar, and Palaniyandi Kuppan. "Improvement in the mechanical properties of neat GFRPs with multi-walled CNTs." *Journal of Materials Research and Technology* 8, no. 1 (2019): 366-376. https://doi.org/10.1016/j.jmrt.2018.02.009

[10] Cha, Jaemin, Joonhui Kim, Seongwoo Ryu, and Soon H. Hong. "Comparison to mechanical properties of epoxy nanocomposites reinforced by functionalized carbon nanotubes and graphene nanoplatelets." *Composites Part B: Engineering* 162 (2019): 283-288. https://doi.org/10.1016/j.compositesb.2018.11.011
[11] Senthil Kumar, M. S., N. Mohana Sundara Raju, P. S. Sampath, and M. Chithirai Pon Selvan. "Influence of nanoclay on mechanical and thermal properties of glass fiber reinforced polymer nanocomposites." *Polymer Composites* 39, no. 6 (2018): 1861-1868. https://doi.org/10.1002/pc.24139
[12] Tze, William TY, Douglas J. Gardner, Carl P. Tripp, and Shane C. O'Neill. "Cellulose fiber/polymer adhesion: effects of fiber/matrix interfacial chemistry on the micromechanics of the interphase." *Journal of adhesion science and technology* 20, no. 15 (2006): 1649-1668. https://doi.org/10.1163/156856106779024427
[13] Selvan, S. Senthamizh, and IS Rajay Vedaraj. "Effects of nanoparticles on the mechanical and thermal behavior of fiber reinforced polymer composites–A review." *Materials Today: Proceedings* (2023). https://doi.org/10.1016/j.matpr.2023.07.008
[14] Vaganov, Gleb, Vladimir Yudin, Jyrki Vuorinen, and Evgeniy Molchanov. "Influence of multiwalled carbon nanotubes on the processing behavior of epoxy powder compositions and on the mechanical properties of their fiber reinforced composites." *Polymer composites* 37, no. 8 (2016): 2377-2383. https://doi.org/10.1002/pc.23419
[15] Yildirim, Ferhat, Mustafa Aydin, and Ahmet Avci. "Improved mechanical performance of three-dimensional woven glass/epoxy spacer composites with carbon nanotubes." *Journal of Reinforced Plastics and Composites* 40, no. 13-14 (2021): 533-549. https://doi.org/10.1177/0731684421990893
[16] Xu, Yuan, and Suong Van Hoa. "Mechanical properties of carbon fiber reinforced epoxy/clay nanocomposites." *Composites Science and Technology* 68, no. 3-4 (2008): 854-861. https://doi.org/10.1016/j.compscitech.2007.08.013
[17] Bortz, Daniel R., Erika Garcia Heras, and Ignacio Martin-Gullon. "Impressive fatigue life and fracture toughness improvements in graphene oxide/epoxy composites." *Macromolecules* 45, no. 1 (2012): 238-245. https://doi.org/10.1021/ma201563k
[18] Parashar, Avinash, and Pierre Mertiny. "Multiscale model to study of fracture toughening in graphene/polymer nanocomposite." *International Journal of Fracture* 179 (2013): 221-228. https://doi.org/10.1007/s10704-012-9779-y
[19] Martin-Gallego, Mario, Raquel Verdejo, Adrian Gestos, Miguel A. Lopez-Manchado, and Qipeng Guo. "Morphology and mechanical properties of nanostructured thermoset/block copolymer blends with carbon nanoparticles." *Composites Part A: Applied Science and Manufacturing* 71 (2015): 136-143. https://doi.org/10.1016/j.compositesa.2015.01.010
[20] Kouassi, A. Y. E., R. Matadi Boumbimba, and M. K. Sangaré. "Effect of the Nanostrength® M53 on Elastic Properties of Glass Fiber Reinforced Acrylic Thermoplastic Resin." In *International Congress for Applied Mechanics*, pp. 1-15. Cham: Springer Nature Switzerland, 2022. https://doi.org/10.1007/978-3-031-49727-8_1
[21] Wang, Lei, Ji Zhou, Haoruo Zhang, Huawei Zou, Yang Chen, Mei Liang, and Zhengguang Heng. "Nanostructure transformation in epoxy/block copolymer composites with good mechanical properties." *Reactive and Functional Polymers* 176 (2022): 105299. https://doi.org/10.1016/j.reactfunctpolym.2022.105299
[22] Bashar, Mohammad T., Uttandaraman Sundararaj, and Pierre Mertiny. "Morphology and mechanical properties of nanostructured acrylic tri-block-copolymer modified epoxy." *Polymer Engineering & Science* 54, no. 5 (2014): 1047-1055. https://doi.org/10.1002/pen.23648
[23] Boumbimba, R. Matadi, Catherine Froustey, Philippe Viot, Jean Marie Olive, Frédéric Léonardi, Pierre Gerard, and Raber Inoubli. "Preparation and mechanical characterisation of laminate composites made of glass fibre/epoxy resin filled with tri bloc copolymers." *Composite structures* 116 (2014): 414-422. https://doi.org/10.1016/j.compstruct.2014.05.028
[24] Liu, Yue, Shusheng Chen, Shibing Ye, and Jiachun Feng. "A feasible route to balance the mechanical properties of epoxy thermosets by reinforcing a PCL-PPC-PCL toughened system with reduced graphene oxide." *Composites Science and Technology* 125 (2016): 108-113. https://doi.org/10.1016/j.compscitech.2016.02.004
[25] Thanh, Nguyen Trung, Nguyen Ba Ngoc, Truong Dinh Tuan, Hoang Ngoc Phuoc, Nguyen Van Huy, and Tran Van Quyen. "Preparation and Properties of Nanocomposite Based on K-153 Epoxy Reinforced T-13 Glass Fiber." *Malaysian Journal on Composites Science and Manufacturing* 10, no. 1 (2023): 1-10. https://doi.org/10.37934/mjcsm.10.1.110
[26] Shah, SZ Hussain, P. S. M. Megat-Yusoff, S. Karuppanan, R. S. Choudhry, Israr Ud Din, A. R. Othman, K. Sharp, and P. Gerard. "Compression and buckling after impact response of resin-infused thermoplastic and thermoset 3D woven composites." *Composites Part B: Engineering* 207 (2021): 108592. https://doi.org/10.1016/j.compositesb.2020.108592

[27] Shah, S. Z. H., Puteri SM Megat Yusoff, Saravanan Karuppanan, and Zubair Sajid. "Elastic constants prediction of 3D fiber-reinforced composites using multiscale homogenization." *Processes* 8, no. 6 (2020): 722. https://doi.org/10.3390/pr8060722

[28] Shah, S. Z. H., Rizwan Saeed Choudhry, and Laraib Alam Khan. "Challenges in compression testing of 3D angle-interlocked woven-glass fabric-reinforced polymeric composites." *Journal of Testing and Evaluation* 45, no. 5 (2017): 1502-1523. https://doi.org/10.1520/JTE20160191

[29] Shah, S. Z. H., P. S. M. Megat-Yusoff, S. Karuppanan, R. S. Choudhry, and Z. Sajid. "Multiscale damage modelling of 3D woven composites under static and impact loads." *Composites Part A: Applied Science and Manufacturing* 151 (2021): 106659. https://doi.org/10.1016/j.compositesa.2021.106659

[30] Shah, S. Z. H., R. S. Choudhry, and Laraib Alam Khan. "Investigation of compressive properties of 3D fiber reinforced polymeric (FRP) composites through combined end and shear loading." *Journal of Mechanical Engineering Research* 7, no. 4 (2015): 34-48. https://doi.org/10.5897/JMER2015.0354

[31] Sajid, Z., S. Karuppanan, K. E. Kee, N. Sallih, and S. Z. H. Shah. "Carbon/basalt hybrid composite bolted joint for improved bearing performance and cost efficiency." *Composite Structures* 275 (2021): 114427. https://doi.org/10.1016/j.compstruct.2021.114427

[32] Malik, Khurshid, Faiz Ahmad, MSI Shaik Dawood, Mohammad S. Islam, Saad Ali, Ali Raza, and Chowdhury Ahmed Shahed. "Mechanical property enhancement of graphene-kenaf-epoxy multiphase composites for automotive applications." *Composites Part A: Applied Science and Manufacturing* 177 (2024): 107916. https://doi.org/10.1016/j.compositesa.2023.107916

[33] Rahim, F. H. A., S. Z. H. Shah, P. S. M. Megat-Yusoff, S. M. Hussnain, R. S. Choudhry, and M. Z. Hussain. "Mechanical and viscoelastic properties of novel resin-infused thermoplastic tri-block copolymer 3D glass fabric composites." *Polymer Testing* 137 (2024): 108510. https://doi.org/10.1016/j.polymertesting.2024.108510

[34] Shah, SZ Hussain, P. S. M. Megat-Yusoff, S. Karuppanan, R. S. Choudhry, F. Ahmad, Z. Sajid, P. Gerard, and K. Sharp. "Performance comparison of resin-infused thermoplastic and thermoset 3D fabric composites under impact loading." *International Journal of Mechanical Sciences* 189 (2021): 105984. https://doi.org/10.1016/j.ijmecsci.2020.105984

[35] Shah, S. Z. H., P. S. M. Megat-Yusoff, R. S. Choudhry, Zubair Sajid, and Israr Ud Din. "Experimental investigation on the quasi-static crush performance of resin-infused thermoplastic 3D fibre-reinforced composites." *Composites Communications* 28 (2021): 100916. https://doi.org/10.1016/j.coco.2021.100916

[36] Shah, Syed Zulfiqar Hussain, Puteri Sri Melor Megat-Yusoff, Saravanan Karuppanan, Rizwan Saeed Choudhry, Faiz Ahmad, and Zubair Sajid. "Mechanical properties and failure mechanisms of novel resin-infused thermoplastic and conventional thermoset 3D fabric composites." *Applied Composite Materials* (2021): 1-31. https://doi.org/10.1007/s10443-021-09980-1

[37] Hussnain, S. M., S. Z. H. Shah, P. S. M. Megat-Yusoff, R. S. Choudhry, and M. Z. Hussain. "Hygrothermal effects on the durability of resin-infused thermoplastic E-glass fiber-reinforced composites in marine environment." *Polymer Composites*. https://doi.org/10.1002/pc.28743

[38] Hafzareen, Nur Md Hanafiah, Abdul Rahim Othman, and Mark Ovinis. "Significant Effect of Vacuum Bagging Processing on Inter-Laminar Shear Strength and Voids of Composite in Oven Cure." *Journal of Advanced Research in Applied Sciences and Engineering Technology* 37, no. 1 (2024): 69-81. http://dx.doi.org/10.37934/araset.37.1.6981

[39] Kit, Fong Mun, Reazul Haq Abdul Haq, Bukhari Manshoor, Mohammad Fahmi Abdul Ghafir, Mohd Nasrull Abdol Rahman, Jörg Hoffmann, Omar Mohd Faizan Marwah, and Rd Khairilhijra'Khirotdin. "Mechanical Properties of Recycled Polyethylene Terephthalate/Polycarbonate/Methylene Diphenyl Diisocyanate (r-PET/PC/MDI) Composite." *Journal of Advanced Research in Applied Mechanics* 120, no. 1 (2024): 1-13. https://doi.org/10.37934/aram.120.1.113

[40] ASTM Committee D-20 on Plastics. Section D20. 70.01. "Standard test methods for density and specific gravity (relative density) of plastics by displacement." American Society for Testing and Materials, 1991.

[41] ASTM, I. "D3171-15; Standard Test Methods for Constituent Content of Composite Materials." *ASTM International: West Conshohocken, PA, USA* (2015).

[42] Standard, ASTM "D 7264/D 7264M–07 Standard Test Method for Flexural Properties of Polymer Matrix Composite Materials." *Annual Book of ASTM Standards* (2007): 1-11.

[43] Rabbi, Sanaul, Snigdha Das, Sanjida Sharmin, and Abdullah Al Mamun. "Effect of nanomaterials on the mechanical and morphological properties of jute-GFRP hybrid nanocomposites." *Malaysian Journal on Composites Science and Manufacturing* 14, no. 1 (2024): 16-33. https://doi.org/10.37934/mjcsm.14.1.1633

[44] Klingler, Andreas, and Bernd Wetzel. "Fatigue crack propagation in triblock copolymer toughened epoxy nanocomposites." *Polymer Engineering & Science* 57, no. 6 (2017): 579-587. https://doi.org/10.1002/pen.24558